Diffuse Reflectance Spectroscopy

JOSÉ TORRENT and VIDAL BARRÓN, University of Córdoba, Spain

The appearance of a soil results from the interaction of its different constituents with incident light. Color and various other attributes of the appearance of soil are highly sensitive to the nature, proportion, particle size and morphology, and spatial association of its mineral and organic components. In fact, color has been used for more than 75 yr to obtain information about these soil properties with a goal of characterizing and distinguishing soil types.

The demand for a standardized method to describe soil color was met by the adoption of the Munsell notation by the USA Soil Survey Program in 1949 and, about 10 yr later, by the International Society of Soil Science (Simonson, 1993). Since then, Munsell Soil Color Charts (Munsell Color, 1975) have been systematically used by pedologists. Visual estimation of soil color, however, is subject to substantial error due to various psychophysical and physical factors. For this reason, the use of colorimeters and spectrophotometers has gained widespread acceptance among soil scientists as a means to measure color accurately and precisely. Moreover, different types of spectrophotometers afford the elucidation of the spectrum of light reflected by a soil illuminated in various ways.

Reflectance, which is the base quantity that characterizes the process of reflection, is defined as the ratio of the reflected radiant flux (or power) to the incident radiant flux (or power) (Wyszecki and Stiles, 1982). Generally, the reflectance of a soil at any wavelength λ can be considered to be the sum of two components: *regular* (or specular, or mirror) reflectance and *diffuse* (or volume or nondirectional) reflectance (defined in more detail below). Reflectance measurements in the field are usually made on relatively large areas (>10 cm^2). Under these conditions, both specular and diffuse reflectance usually contribute to the total reflectance of a soil surface, the magnitude of which depends on particle size, structure, microrelief, and other properties that define the "surface state" (Escadafal, 1989). In contrast, laboratory measurements of soil reflectance are usually made on small areas (<10 cm^2) of disturbed soil materials that are usually sieved or ground to a small size. In this case diffuse reflectance predominates, which depends mainly on soil composition.

This chapter describes available laboratory methods for recording diffuse reflectance spectra for soil materials and ways to handle the information to identify and characterize soil minerals. Only the visible and narrow vicinal ultraviolet (UV) and infrared (IR) regions of the spectrum are considered here because reflectance in the IR region is the subject of another chapter (Johnston and Aochi, 1996)).

Methods of Soil Analysis. Part 5. Mineralogical Methods. SSSA Book Series, no. 5.

PRINCIPLES

A brief introduction to the theoretical principles of diffuse reflection is provided here. For an in-depth description of this phenomenon, interested readers are referred to textbooks such as those of Wendlandt and Hecht (1966), Kortüm (1969), Wyszecki and Stiles (1982), and Hapke (1993).

A beam of light impinging on a flat polished surface of a crystal larger than the beam cross section is partly specularly reflected and partly refracted following the laws of geometric optics (contained in the Fresnel equations). In absorbing materials, the radiant flux is absorbed according to the well-known Lambert Absorption Law:

$$I = I_0 e^{-K_T x} \qquad [1]$$

where I is the radiation flux transmitted from an initial flux I_0 following passage through a layer of thickness x of a medium with an absorption (or extinction) coefficient K_T measured in transmission.

When the dimensions of the particle are small compared with the beam cross section but large relative to the light wavelength, diffraction phenomena also occur because rays striking the crystal and passing by it result in interferences among elementary waves. In powders of randomly oriented particles of such size, part of the incident light goes back at all angles into the hemisphere of provenance of the light. The phenomenon resulting from the reflection, refraction, diffraction, and absorption by particles oriented in all directions is called *diffuse* (or *volume*) *reflection*, in contrast with *regular* (or *directional*) reflection from a plane phase boundary. For ideal diffuse reflection, the angular distribution of reflected light is independent of the angle of incidence and obeys the Lambert Cosine Law. This law states that the remitted radiation per unit surface and unit solid angle is proportional to the cosine of the angle i of incident light and the cosine of the angle of observation, e. There is no such thing as an ideal diffuse reflector, but near-Lambertian behavior is normally observed in tightly pressed powder samples.

If the dimensions of the particle are similar to, or smaller than, the wavelength, then the contributions of reflection, refraction, and diffraction to the intensity and angular distribution of the remitted radiation flux are comparable and impossible to separate. The phenomenon is then designated as *scattering*. Various theories have provided a reasonably solid basis to interpret single scattering by isolated molecules of absorbing or nonabsorbing isotropic particles. However, as the distance between particles decreases, single scattering gives way to *multiple scattering*, which logically predominates in densely packed crystal powders and pigment mixtures.

The angular distribution of light scattered by a single particle is far from isotropic. On the other hand, simple semiquantitative investigations have shown that, with sufficiently large number of particles and layer thickness, an isotropic distribution eventually arises within the sample (Kortüm, 1969). Essentially, this corresponds to diffusely reflected radiation for a layer of densely packed coarse particles, for which, as stated above, the laws of reflection, refraction, diffraction, and absorption still hold. Support for this assumption is provided by the experimentally confirmed validity of the Lambert Cosine Law for multiple scattering by fine particles.

There is no general quantitative solution to the problem of multiple scattering. Purely phenomenological theories have thus been developed to describe the system properties. Several theories are based on two constants that characterize the absorption and scatter-

ing per unit layer thickness of the medium. These so-called *coefficients of absorption* and *scattering* are generally taken to be properties of the irradiated layer, assumed to be a continuum, and are experimentally accessible.

The Kubelka–Munk Theory

The Kubelka and Munk (1931) theory assumes that a plane-parallel layer of thickness X capable of both scattering and absorbing radiation is irradiated in the $-x$ direction with a diffuse monochromatic radiation flux I (Fig. 13–1). The layer is very extensive relative to X and can be split into infinitesimal layers of thickness dx. The diffuse radiation flux in the negative and positive x directions are designated I and J, respectively. If, in passing through dx, the downward flux I is decreased by an amount KIdx by absorption, and increased by an amount SIdx by scattering, and a similar reasoning is made for the upward flux J, then the following differential equations can be derived:

$$\frac{-\mathrm{d}I}{\mathrm{d}x} = -(K+S)I + SJ \qquad [2]$$

$$\frac{\mathrm{d}J}{\mathrm{d}x} = -(K+S)J + SI \qquad [3]$$

where K and S are the absorption and scattering coefficient of the sample, respectively.

Kubelka (1948) obtained explicit hyperbolic solutions to this equation that were discussed in detail by Wyszecki and Stiles (1982). The most general solution is

$$R = \frac{1 - R_g(a - b\coth bSX)}{a - R_g + b\coth bSX} \qquad [4]$$

where R is the reflectance of the layer over a background of reflectance R_g, cothbSX the hyperbolic cotangent of bSX, X the layer thickness, $a = 1 + K/S$, and $b = (a^2 - 1)^{0.5}$.

Routinely, many measurements are made on layers thick enough to ensure that a further increase in thickness will fail to change the reflectance. Under these conditions, the reflectance is given by R_∞ and Eq. [4] yields

$$\frac{K}{S} = \frac{(1 - R_\infty)^2}{2R_\infty} = F(R_\infty) \qquad [5]$$

where $F(R_\infty)$ is usually termed the *remission* or *Kubelka–Munk* (*K–M*) *function*.

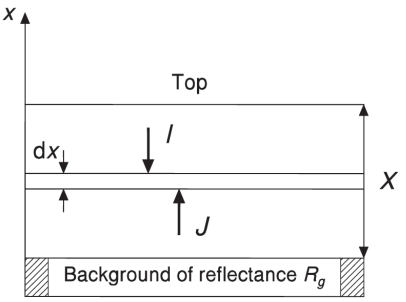

Fig. 13–1. Cross-sectional diagram of a powder layer.

It must be noted that the reflectance at any wavelength is a function of the K/S ratio rather than of the absolute values of K and S. As a result, these two absolute values cannot be obtained from Eq. [5].

The validity of Eq. [5] has been tested through carefully designed measurements on samples of colored glass for which the scattering coefficient was shown to be independent of the wavelength, and both K (Eq. [5]) and K_T (the absorption coefficient in transmission, Eq. [1]) were measured. K was found to be proportional to K_T by a factor similar at all wavelengths (Kortüm, 1969). Hence, the logarithmically plotted reflectance spectrum could be vertically offset to make it coincide with the logarithmically plotted transmission spectrum. For this reason, either $F(R_\infty)$ or the apparent absorbance $[\log(1/R_\infty)]$ are proxies for the actual absorption spectrum. Such a significant finding has been used to identify the characteristic absorption bands of minerals (Sherman and Waite, 1985; Burns, 1993).

As noted, the "typical" absorption spectrum constructed from reflectance measurements [i.e., the $F(R_\infty)$ curves] should reflect the true absorption spectrum only if the scattering coefficient is independent of the wavelength. This is only the case when the average grain size is large relative to the wavelength. Otherwise, the scattering coefficient usually decreases with increasing wavelength. Exceedingly coarse grains pose other problems (heterogeneity of the mixture and significant regular reflection) that greatly reduce differences between maxima and minima in the absorbance curves. For this reason, fine-grained (0.1–1 μm) samples are preferred, even though the decrease in scattering coefficient with increasing wavelength results in a flattening of the typical color curves toward the UV region and a "red-shift" of maxima in the color curve.

The dependence of the K–M function or the apparent absorbance $[\log(1/R_\infty)]$ on particle size is rather complex, particularly in heterogeneous mixtures such as ground soil materials, where both particle size range and differences in absorption coefficient among minerals are wide. The absorption coefficient (either K or K_T) invariably decreases with increasing particle size throughout the size range of interest, and the spectrum flattens. However, differences between weak and strongly absorbing materials continue to exist as relates to the size-dependence of absorbance. In strongly absorbing materials, absorbance increases with decreasing particle size for sizes smaller than the wavelength through an increased absorption coefficient. With particle sizes larger than the wavelength, the absorbance also usually decreases with increasing particle size because (i) the fraction of regular reflection increases with increasing particle size and (ii), as predicted by the Fresnel equations, regular reflection has much weight in strongly absorbing materials. In weakly absorbing materials, on the other hand, an increase in particle size above the wavelength results in an increase in absorbance because the decrease in K is offset by that in S (which is proportional to the reciprocal of particle size). Because K is small, light can penetrate deeper into the sample and increase the absorbance.

In summary, the K–M theory allows one to obtain the typical absorption spectrum for an absorbing mineral or mineral mixture, but one must consider those factors affecting the curve. In practice, significant deviations from the theory occur at $R_\infty < 0.6$. For this reason, dilution of the sample to be measured with a "white" standard possessing a known scattering coefficient at the different wavelengths has usually been recommended. K values can then be calculated from the K–M function on the proven assumption that the scattering coefficient of the diluted sample can be approximated by that of the diluent. Absolute values of S can be determined by measuring the reflectance of several mounts consisting of thin layers of standard against a background of reflectance $R_g = 0$. S can then be obtained from the slope of the plot against thickness, X, of the following function:

$$SX = \frac{1}{b}\coth^{-1}\frac{1 - aR_0}{bR_0} \quad [6]$$

where a and b are defined as for Eq. [4], and R_0 is the reflectance in front of the black background.

The *K–M* theory has been criticized on several fronts, namely: misinterpretation of the K and S parameters because they are mutually dependent, lack of physical meaning of the reflectance because it can be measured in different ways, and poor definition of parameter S. In addition, the practice of diluting the sample with a white standard to prevent saturation of the remission function may not be effective (Hapke, 1993).

Recent Theories

In the early 1980s new theories were developed that provided solutions to the problem of radiative transfer in a complex particulate medium. The simplest of such theories was that of Hapke (1981, 1993), in which the primary quantity in reflectance is not the remission function, but the *particle single-scattering albedo, w*. This represents the probability of a photon surviving an interaction with a single particle (i.e., the ratio of the total amount of power scattered/total power removed from the wave). For particulate media, the *volume single-scattering albedo*, $\bar{w}$, is the average of the single-scattering albedo for the individual particles. The theory starts with the formalism of the equation of radiative transfer, which is used to determine how the intensity of an electromagnetic wave is changed by the processes of emission, absorption, and scattering as the wave propagates through a complex medium. Hapke coined the term *diffusive reflectance* to designate the reflectance derived from the simplest two-stream solution to the radiative transfer equation. This diffusive reflectance has no physical meaning (*K–M* is in fact a form of diffusive reflectance) and is defined on the assumption that the radiation impinges on a plane corresponding to $z = 0$ that separates an empty half-space from an infinitely thick lower half-space filled with particles that scatter and absorb light. The assumptions in the diffusive reflectance formalism are that the incident radiance does not penetrate into the medium, but rather acts as if the upper boundary were covered by an invisible membrane scattering incident light uniformly in all downward directions, and that no sources of radiation exist within this medium. The problem is then to determine the radiance in the medium and the scattered radiance emerging from the $z = 0$ plane in the upward direction into the half-space. In the two-stream approximation, the solid angle is entirely occupied by the upward- and the downward-going hemispheres.

Hapke (1981) derived a relation between the particle single-scattering albedo, the complex index of refraction, the grain size, and a scattering parameter to describe scattering centers within imperfect grains. For the case of volume single-scattering albedo of isotropic scatterers, he developed analytical approximations for the different cases of reflectance (measured relative to a white standard). For the diffusive reflectance, the expression was

$$\bar{w} = \frac{4R}{(1 + R)^2} \quad [7]$$

Because diffusive reflectance lacks physical meaning, this equation is only of use for rapid semiquantative estimation of $\bar{w}$. A variety reflectance types exists in terms of spectrophotometric measurements that depend on the degree of collimation of the light

source and detector, the usual attributes used being *directional*, *conical* and *hemispherical*. As signaled by Hapke (1993), all measured reflectances are biconical because neither perfect collimation nor perfect diffuseness can be achieved in practice. In the particular case of directional-hemispherical reflectance (where the object is illuminated by a highly collimated source and the total amount diffuse light scattered into the upward hemisphere is measured, $\bar{w}$ is given by

$$\bar{w} = \frac{R^2\left(4\cos^2 i - 1\right) + R\left(4\cos i + 2\right)}{(1 + 2R\cos i)^2} \qquad [8]$$

in which i is the incidence angle. When $i = 0$, Eq. [8] reduces to

$$\bar{w} = \frac{3R^2 + 6R}{(1 + 2R)^2} \qquad [9]$$

Equations [8] and [9] have been successfully used to estimate the absorption coefficients of minerals and for quantitative analysis, as discussed later in this chapter.

Analysis of Mixed Powders

Duncan (1940, 1949) showed the absorption and scattering coefficients of a mixture to be simple additive functions of the respective coefficients of the mixture components weighed according to their proportions. Hence, the *K–M* function for the mixture can be written as

$$F(R_M) = \frac{(1 - R_M)^2}{2R_M} = \left(\frac{K}{S}\right)_M = \frac{\sum C_i K_i}{\sum C_i S_i} \qquad [10]$$

where subscript M refers to the mixture, R_M is R_∞ for the mixture, and C_i is the mass fraction of component i with absorption coefficient K_i and scattering coefficient S_i.

Equation [10], which is frequently used in quantitative analysis, can be further simplified for mixtures containing a large excess of a diluent such that the scattering coefficient is completely dictated by the diluent:

$$F(R_M) = \frac{1}{S}\sum C_i K_i \qquad [11]$$

Equation [10] can also be used to determine the K and S values for a single- or multimineral sample, K_p and S_p. For this purpose, the sample is mixed with variable amounts of an appropriate white standard, ST, whose reflectance is set to 1 (i.e., $K_{st} = 0$, according to Eq. [5]). Equation [10] for any mixture thus becomes

$$F(R_M) = \frac{(1 - R_M)^2}{2R_M} = \frac{C_p K_p + C_{st} K_{st}}{C_p S_p + C_{st} S_{st}} = \frac{C_p K_p}{C_p S_p + C_{st} S_{st}} \qquad [12]$$

which can be expressed as

$$\frac{2R_M}{(1 - R_M)^2} = \frac{S_p}{K_p} + \frac{C_{st}}{C_p}\frac{S_{st}}{K_p} \qquad [13]$$

By plotting the left-hand side of Eq. [10] against C_{st}/C_p for different mixtures, the slope of the regression line gives S_{st}/K_p and the intercept S_p/K_p. For simplicity, a value of $S_{st} = 1$ is usually adopted whereby relative rather than absolute values of S_p are obtained. In this way, Eq. [13] yields K_p and S_p at any wavelength.

One alternative analysis not suffering from some of the drawbacks of the *K–M* approach is based on the volume single-scattering albedo. According to Hapke (1981), the value of this variable for a multimineral surface, $\bar{w}_M$, is given by

$$\bar{w}_M = \frac{\sum(C_i w_i / \rho_i d_i)}{\sum(C_i / \rho_i d_i)} \qquad [14]$$

where i denotes the ith component, C_i the mass fraction, ρ_i the density of the mineral, d_i the mean grain diameter, and w_i the single scattering albedo of the ith component.

Color Notation and Calculations

Torrent and Barrón (1993) provided a brief introduction to soil color and its laboratory measurement, and Wyszecki and Stiles (1982) supplied a comprehensive treatment of colorimetric concepts. Here, it suffices to say that the diffuse reflectance spectrum in the visible region allows one to numerically specify the color of a soil or mineral mixture.

Briefly, color notation is based on an empirical thrichromatic generalization. In psychophysical terms, any color can be identified by only three color stimuli, a *color stimulus* being radiant energy of a given intensity and spectral composition entering the eye and producing a sensation of color. Therefore, any spectrum reaching the observer's eye can be converted into the so-called *tristimulus* values, designated *X*, *Y*, and *Z*. For this purpose, the so-called *standard observer*, that is, the "ideal" observer established by the Commission Internationale de l'Eclairage (CIE) in 1931, is considered. Tristimulus values result from the combination of the reflectance spectrum of the observed object with the spectrum of the illuminating light. *X*, *Y*, and *Z* must thus be defined with reference to a standard illuminant.

Color can be specified by using *X*, *Y*, and *Z*, or the *chromaticity coordinates*, $x = X/(X + Y + Z)$, $y = Y/(X + Y + Z)$, which, together with *Y*, define a region of well-defined limits or *color solid* in a three-dimensional space. Generally, other color spaces that are more uniform in psychophysical terms are used, the coordinates of which are calculated from *X*, *Y*, and *Z* (which are calculated, in turn, from the reflectance spectrum). Soil and other earth scientists use the part of the Munsell Color Space represented in Munsell Soil Color Charts (Munsell Color, 1975). The coordinates of this system are designated with the familiar terms *hue*, *value*, and *chroma*. One useful alternative system is the CIE 1976 ($L^*a^*b^*$) space (Commission Internationale de L'Eclairage, 1978), which is based on the coordinates lightness (L^*), redness–greenness ($+a^* \rightarrow -a^*$) and yellowness–blueness ($+b^* \rightarrow -b^*$).

METHODS

Apparatus

Diffuse reflectance measurements are usually made by using a UV-visible spectrophotometer equipped with a diffuse reflectance accessory (integrating sphere) capable of collecting the reflected flux. Currently, many high-performance, research spectrophotometers can be fitted with an integrating sphere/detector module, which usually replaces the cell

holders used for transmission measurements in the measuring compartment. Commercial sources[1] of these spectropohotometers include PerkinElmer Analytical Instruments (Norwalk, Connecticut), Shimadzu Scientific Instruments, Inc. (Columbia, Maryland), and Varian, Inc. (Palo Alto, California). Integrating spheres adaptable to different spectrophotometers are supplied by Labsphere (North Sutton, New Hampshire) and others.

An integrating sphere is essentially a hollow sphere internally coated with a white material of diffuse reflectance close to 1. The sphere has apertures through which a beam of radiant energy can penetrate and ports for mounting samples and standards and placing the appropriate detectors. Commercially available spheres range from 50 to 250 mm in diameter and are internally coated with highly diffusing polytetrafluoroethylene (PTFE) or barium sulfate ($BaSO_4$). Their performance increases with increasing diameter and decreasing port fraction. As a general rule, no more than 5% of the sphere surface area should be occupied by port openings.

As discussed above, the *K–M* and other forms of diffusive reflectance are strictly mathematical artifices with no direct physical meaning. In practice, however, reflectance measurements are performed under specific geometric conditions. For instance, under the specific hemispherical–directional reflectance conditions illustrated in Fig. 13–2a, reflectance is measured by illuminating the sample with diffuse light (generated by a beam of incident light impinging on a spot of the sphere surface), the angle between the normal to the sample surface and the axis of the viewing beam not exceeding 10°. Most commercial spectrophotometers measure directional–hemispherical reflectance, whereby the sample is illuminated by a beam whose axis does not depart by more than 10° from the normal to the sample and the reflected radiation collected by the sphere goes to the detector (Fig. 13–2b). Some instruments possess cylindrical (ring) integrating surfaces where measurements are made under the 45/0 or the 0/45 conditions, which are analogous to the diff/0 or 0/diff conditions illustrated in Fig. 13–2 but with the illuminating or the viewing beam at 45 ± 5° to the normal to the sample. Integrating spheres usually contain small baffles placed between the sample and the area of the sphere that is illuminated or viewed. These baffles prevent directly reflected light from superimposing on the illuminated sample or on the area of the surface that is being viewed.

Standards

The perfect reflecting diffuser, defined as the ideal uniform diffuser with reflectance equal to 1, does not exist in nature, as discussed above, so the white standards used in

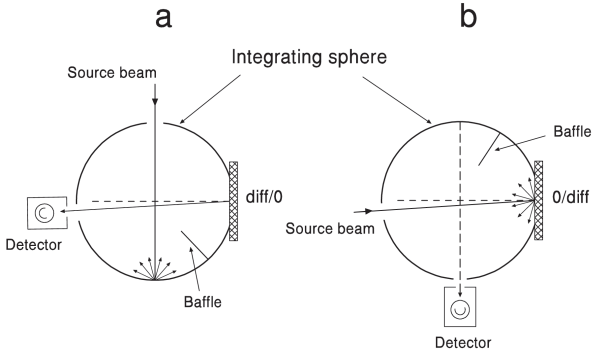

Fig. 13–2. Schematic diagrams showing (a) the diff/0, and (b) the 0/diff standard illuminating and viewing geometries in an integrating sphere.

[1] Reference to trade and company names is purely for the convenience of the reader and does not imply endorsement by the Universidad de Córdoba, nor that similar products may not be satisfactory.

diffuse reflectance measurements are secondary standards from which the reflectance is known by means of special calibration procedures (Wyszecki and Stiles, 1982).

Smoked magnesium oxide (MgO) was used as a standard for many years because its absolute reflectance in the visible range is close to 0.98. At present, barium sulfate and halon (PTFE) are considered suitable standards by the CIE. The Merck DIN 5033 barium sulfate powder standard (EM Industries Inc., Hawthorne, NY) has an absolute reflectance of 0.973 to 0.988 in the 380- to 750-nm wavelength range, and >0.95 in the 750- to 1500-nm wavelength range. When used as a spectrophotometric standard, it must be pressed to 2 g cm^{-3} (ASTM, 1973). Halon has a microcrystalline structure formed under pressure and excellent reflectance properties. Pressed tablets of halon, available under the trade name of Spectralon (Labsphere, North Sutton, NH) are washable and exhibit reflectance values >0.99 in the 400- to 1500-nm wavelength range, and >0.95 in the 250- to 2500-nm wavelength range.

Materials suitable for working standards include some opal glasses, ceramic plates, and various powder mixtures. However, they require periodic recalibration since dust, moisture, and exposure to radiation affect their optical properties. In practice, the use of barium sulfate as described below is convenient for most applications.

Sample Preparation

Diffuse reflectance spectra are significantly sensitive to the manner in which the soil or mineral mixture sample is prepared. There is no universal best procedure for this purpose. The operator must thus carefully consider the factors potentially influencing those features of the spectrum from which useful information is to be derived.

Particle size is the factor most strongly affecting reflectance, as shown by the occasionally dramatic changes in soil color upon grinding. For the reasons discussed above (mainly sample heterogeneity and regular reflection), the best results are obtained with small particle sizes, so it is generally advisable to grind the sample to a fine silt (<10 μm) size. For sandy samples, this may result in a dramatic increase in lightness and fading of colors due to coloring minerals, which are diluted in the mass of fine particles produced by grinding of sand. Despite this apparent drawback, most spectral features of interest are usually preserved after grinding.

The grinding procedure and intensity influence the spectrum for the end product. The fast and effective grinding provided by ball mills is not always advisable because, above a certain grinding energy, some minerals are transformed into others (e.g., goethite becomes hematite). Also, amorphous coatings may be formed on the surface of some minerals. Consistent results and preservation of the spectral features of interest can be achieved in most instances simply by grinding the sample in an agate mortar, so that minerals are in the volume-scattering region. Barrón and Torrent (1986) used a grinding time of 10 min in the agate mortar for samples of about 0.5 g; further grinding caused only minor changes in the spectral features of the samples.

Preferential orientation of particles of layer silicates, and occasionally other minerals (e.g., feldspars), must be avoided because it results in regular reflection, thus breaking the laws of diffuse reflection. For this reason, the soil powder is usually pressed against a rough surface such as frosted glass or unglazed paper. Dilution of the sample with a barium sulfate standard usually reduces preferential orientation to an acceptable minimum. On the other hand, preferential orientation can be advantageously used to detect low proportions of minerals with platy morphology (as is the case with oriented mounts in X-ray diffraction). This has scarcely been used in practice, however.

Moist soil samples have occasionally been used, particularly by pedologists interested in observing color changes upon moistening. Moist pastes can be prepared by adding the desired proportion of water to the soil sample according to the previously determined moisture content at different suction pressures. Moisture loss during measurement, which can be a major source of error, must be evaluated by measuring the sample spectrum at variable intervals. Bedidi et al. (1992) showed the diffuse reflectance spectrum for a soil to undergo nonlinear changes with increasing moisture content. Therefore, the spectral signatures of moist soils usually cannot be derived from those of their dry counterparts.

Sample Holders

Instrument manufacturers have provided a variety of sample holders that can be adapted to the sample ports of different integrating spheres or ring collectors. Many holders possess a cover glass to prevent loose powder from falling into, and damaging, the integrating sphere when sample ports are vertical or horizontally positioned on top of the sphere. Because cover glasses cause substantial qualitative deviations from the *K–M* theory (Kortüm, 1969), only special reasons justify their use. Therefore, the only choice available with vertical ports is to use self-supporting pressed powder mounts. Preparation of these mounts requires that the powder be fine and that the area of the holder hole be relatively small. Rectangular or ovalated holes with a maximum size of 8 to 10 by 12 to 16 mm are usually suitable. The minimum size is logically the viewing area of the spectrophotometer, which is in the region of several tens of a square millimeter in most instruments. Fernandez and Schulze (1987) used Plexiglas 44 by 44 by 13 mm holders with a 20 by 8 mm hole with rounded ends to prevent samples from sticking in the corners and to facilitate cleaning. Sample holders with a hole of appropriate size and external dimensions for placement in the allocated space on the port area can be cut out from boards of various opaque plastic materials. Preferably, the surface of these boards should lack gloss, which can be ensured by abrading the surface with corundum powder.

Portable spectrophotometers allow the rapid measurement of the reflectance of unaltered soil surfaces or ground soil samples without the need for special preparation. However, they generally measure reflectance at relatively large wavelength steps. This restricts detailed band analysis and quantitative calculations.

Acquisition of Reflectance Spectra

Materials

- Agate mortar (60–70 mm diameter).
- Reference standards (disks of Spectralon or pressed barium sulfate).
- Standard barium sulfate powder (Merck DIN 5033 or similar).
- Two sample holders and a plunger adapted to the size of the holder hole.
- 5. 2 g of the soil or mineral sample ground to <2 mm or finer.

Procedure

Position the diffuse reflectance accessory in the sample compartment of the spectrophotometer and plug it in. Align the optical system according to the manufacture's operating instructions and let the instrument warm up for a few minutes. Set up the measuring program: wavelength range(s) of interest, mode (reflectance or absorbance), double beam, and scan speed.

When the instrument is ready, place one of the reference disks over the sample port and the other over the reference port. Alternatively, prepare two standards from barium sulfate powder. To do this, place the holder over a frosted plate glass or a flat surface covered with unglazed paper. Add the required amount of barium sulfate powder in several layers and distribute it uniformly in the hole. Press it firmly with the plunger to obtain the required packing density (>2 g cm^{-3}) and a thickness >3 mm. Remove the plunger and check that the barium sulfate surface is perfectly flat—this is required to minimize phase angle effects. Remove loose particles remaining on the surface with the aid of a gentle jet of filtered dry air before placing the holder over the instrument port.

Collect the baseline scan with the standard in place and replace the standard on the sample port with the soil sample. This must be prepared previously by grinding 2 g of the <2-mm sample in the agate mortar for 3 min. Then, take a subsample of 200 to 500 mg (depending on the size of the holder hole) and grind it for 8 to 10 min, or until any apparent grittiness disappears and further grinding causes no apparent color change. Press the resulting powder into the holder hole, as for the barium sulfate powder, to a minimum thickness of 3 mm. Place the holder on the sample port, and record the spectrum.

Unless time for spectrum acquisition is limited, it is recommended for most purposes to obtain reflectance measurements in 0.5- to 1-nm steps for instruments with a wavelength bandwidth of 2 nm. This can take 10 to 20 min for the visible (380–750 nm) range, or 20 to 30 min for the visible-near IR range, in most spectrophotometers.

Comments

If barium sulfate is used as standard, it is advisable to prepare "fresh" standards before each set of measurements. The use of permanent disks saves time, but they tend to lose their reflectance properties with time and necessitate replacing (or washing and polishing).

Special care must be exercised to ensure stability of the powder mount in vertically placed sample holders with no cover glass.

Analysis and Parameterization of Reflectance Spectra

Data Storage

Modern spectrophotometers are computerized, so they allow reflectance data (and the results of various mathematical calculations on them) to be saved in suitable formats. ASCII files are convenient for most applications and can be easily transformed into the file types utilized by common software.

Color Calculations

The visible portion of the spectrum is used to calculate the tristimulus values by multiplying the reflectance values by the values of the so-called *color-matching functions*, which have been tabulated for different illuminants by Wyszecki and Stiles (1982). In the past this was done manually, now software provided by spectrophotometer manufacturers allows much faster calculation. Many software packages also provide conversion of the *X*, *Y*, and *Z* values to the Munsell and CIE 1976 ($L^*a^*b^*$) notations. These conversions can also be made with free software that can be downloaded from the Gretagmacbeth & Munsell Color's site (New Windsor, NY; www.gretagmacbeth.com/index/products/products_colorstandards.htm [verified 26 Mar. 2007]).

Analysis of Absorption Bands

As stated above, the typical absorption spectrum for a soil sample can be approximated by the absorption coefficient, K, in the K–M function. To calculate K, Eq. [13] is used once the reflectances for several mixtures of the sample with a white standard have been obtained. One can use either the absorbance ($\log 1/R_\infty$) or the K–M function [i.e., $F(R_\infty) = (1 - R_\infty)^2/2R_\infty$] as a proxy for the typical absorption spectrum. Although both functions have been used to identify and characterize soil minerals, the latter is preferred for theoretical reasons.

K, absorbance, or K–M spectra can be deconvoluted by using Gaussian functions of the form:

$$\varphi(\lambda) = \sum_{i=1}^{n} h_i \exp\left[4\ln(2)\left(\frac{\lambda - \lambda_i}{\mathrm{FWHH}_i}\right)^2\right] \qquad [15]$$

where $\varphi(\lambda)$ is the spectral function; λ is wavelength (alternatively, wave number can be used); and h_i, λ_i, and FWHH_i are the height, position and full width at half height of the i band, respectively. Scheinost et al. (1999b) successfully applied the Marquardt nonlinear regression method (SAS Institute, 1988) to spectra of absorbance against wavelength. Sunshine et al. (1990) found a modified Gaussian model better than the frequently used Gaussian model to deconvolute absorption bands in complex mixtures of pyroxenes and olivine.

Clark and Roush (1984) successfully used the concept of *continuum* to isolate particular absorption features for the analysis of spectra. The continuum is the "background absorption" onto which other absorption features are superimposed and represents either the absorption due to a different process in a specific mineral or absorption from a different mineral in a mixture. Continua can be modeled in terms of the mean optical path length through different minerals (or separated into different absorption processes) using the equation

$$\exp\left[-k\bar{l}\right] = \exp\left(-\sum_{i=1}^{i} k_i \bar{l}_i\right) \qquad [16]$$

where k and $\bar{l}$ are the equivalent absorption coefficients and mean optical path lengths, respectively, for the surface as a whole, k_i is the absorption coefficient of the ith mineral (or particular absorption process) having a mean optical path length $\bar{l}_i$ for a multimineralic surface in an intimate mixture. Because of its definition, the continuum should be removed by subtraction from apparent absorbance and remission spectra but by division in reflectance spectra.

Direct resolution of the absorption spectra is hardly ever straightforward, so a number of ad hoc assumptions are frequently needed. In practice, different mathematical transformations of the spectra (or their proxies) make band resolution easier. The most widely used transformations are the first and, especially, second derivative. The first derivative of a Gaussian band has a maximum and a minimum to the left and right, respectively, of the maximum in the original band. The difference in ordinate between the maximum and minimum is proportional to the band amplitude. Unfortunately, when bands overlap, the wavelength at which the derivative is zero may be shifted relative to the true band position, or the derivative may not reach a zero value.

The second-derivative curve exhibits a minimum at the point of maximum curvature (i.e., the peak) in the original absorption band. The second-derivative curve provides more information than does the first-derivative curve because the original band, even when overlapped with other bands and not yielding a true absorption maximum (reflectance minimum), always yields a minimum in that curve. Figure 13–3 illustrates this important feature for a soil containing significant amounts of goethite and hematite as main pigments (and yielding bands in the visible region). Second-derivative diffuse reflectance spectroscopy has thus become a powerful tool for identifying and characterizing colored soil minerals (Kosmas et al., 1984, 1986; Scheinost et al., 1998).

Because spectra are acquired stepwise, they must usually be smoothed for calculation of their successive derivatives. Various algorithms are available for this purpose. The cubic spline fitting procedure (Press et al., 1992) involves joining end-to-end a number of cubic polynomial segments. Each segment is based on a certain number of adjacent data points, with the restriction that continuity in the first and second derivative must exist at the joints. The method of Savitzky and Golay (1964) uses least-squares methodology to fit a polynomial curve to a set of contiguous data points (usually from 13 to 31) and calculates the ordinate at the central value of the abscissa (wavelength). A new polynomial curve is then obtained by moving the set one point and calculating the new ordinate. For each polynomial, the slope at the central value of the abscissa gives the derivative. The number of

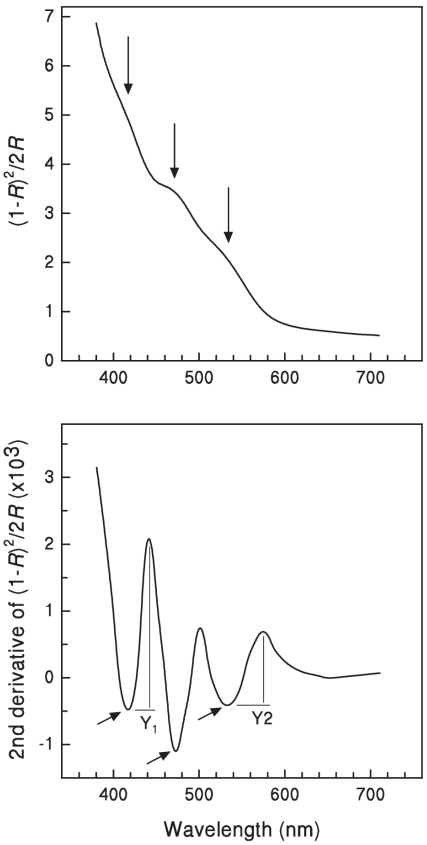

Fig. 13–3. (upper) Kubelka–Munk function spectrum and (lower) its second derivative for a Brazilian Oxisol containing hematite and goethite. The relatively inconspicuous absorption bands (marked with arrows) in the original spectra appear as strong minima in the second-derivative spectrum. The amplitudes of the bands between the minimum at ~415 nm and the maximum at ~445 nm (Y_1) and between the minimum at ~535 nm and the maximum ~580 nm (Y_2) were used in the quantitative analysis of these two minerals.

points in each set is a crucial input parameter in both procedures. Goodness of fit increases, but the degree of smoothing decreases (and resolution coarsens) with decreasing number of points, so a compromise must be adopted. Gálvez et al. (1999) found 22 points to provide the best results when applying a cubic spline procedure to spectra recorded in 0.5-nm steps. Software for smoothing and derivative calculations can usually be obtained from instrument manufacturers and used with little proficiency in mathematics.

APPLICATIONS

Identification of Mineral Species

Some common soil minerals can be identified by their characteristic bands in the absorbance or *K–M* function spectra. Spectral libraries, such as that of the USGS (2003) provide reflectance spectra of the different minerals usually found in soils.

By far, iron oxides have been the most intensively examined soil minerals to date. This is not surprising because together with organic compounds, they constitute the most important soil pigments. They exhibit absorption bands in the UV to near IR wavelength range that are due to the following electronic transitions within the $3d^5$ shell of Fe^{3+} ion: (i) Fe^{3+} ligand field transitions, (ii) transitions due to magnetically coupled Fe^{3+} cations at adjacent sites, and (iii) ligand-to-metal charge transfer. On the basis of the ligand field theory, Sherman and Waite (1985) assigned three bands to the following ligand field transitions: $^6A_1(^6S) \rightarrow {}^4T_1(^4G)$, $^6A_1(^6S) \rightarrow {}^4T_2(^4G)$, and $^6A_1\ (^6S) \rightarrow {}^4E;{}^4A_1(^4G)$. A fourth band was assigned to the electron pair transition or $^6A_1(^6S)$ double exciton $2(^6A_1) \rightarrow 2[{}^4T_1(^4G)]$. This double exciton process usually yields the strongest band, so it exerts a decisive influence on hue. Thus, goethite is yellow and hematite is red because the corresponding band lies at a shorter wavelength in the former (~480 nm) than in the latter (~535 nm).

Scheinost et al. (1998) used the second derivative of the *K–M* function to examine the intensity of these four bands for 176 synthetic and natural Fe oxide samples. They found significant differences in band position and intensity among the eight minerals studied and also among different samples of each mineral. These differences are the result of (i) $Fe(O, OH)_6$ octahedra being linked in different ways, (ii) distortion of the octahedra decreasing symmetry and hence altering the ligand field and band positions, and (iii) differences in the Fe-to-Fe distance and in the degree of occupancy of octahedra likely affecting magnetic coupling of neighboring Fe^{3+} ions and hence the position and intensity of the double exciton band. The combined effect of these factors results in substantial overlap of the bands for different oxides, as shown in Fig. 13–4. Thus, Scheinost et al. (1998) found that (i) pure samples of goethite, maghemite, and schwertmannite could not be discriminated; (ii) at least 80% of pure akagenéite, feroxyhyte, ferrihydrite, hematite, and lepidocrocite samples were correctly classed by using discriminant functions; and (iii) in soil mixtures containing other Fe oxides, only hematite and magnetite could be discriminated from other Fe oxides. Band overlap can thus hinder Fe oxide identification by diffuse reflectance spectroscopy. For instance, this problem, together with poor spectral resolution, has precluded positive identification of Fe oxides in Martian soils and dust (Bell et al., 2000).

Detection limits in second-derivative diffuse reflectance spectroscopy are typically lower than in alternative identification techniques for Fe oxides. Thus, <0.1% goethite and hematite can be detected in mixtures with other soil minerals (Scheinost et al., 1998), and the same applies to Ti oxides (Malengreau et al., 1995). This proportion is more than one order of magnitude smaller than the detection limit of ordinary X-ray diffraction. Low detection limits are also provided by first-derivative spectroscopy (Deaton and Balsam, 1991).

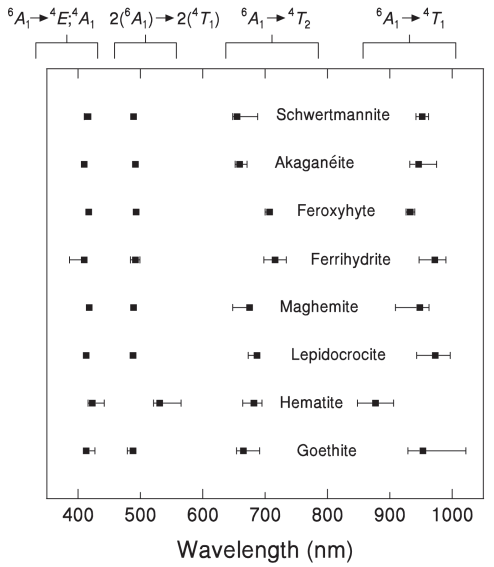

Fig. 13–4. Median and range of the crystal field band positions as determined from second-derivative minima. Adapted from Scheinost el al. (1998).

Elucidation of Crystal Properties

The decisive influence of crystal parameters on the position and intensity of the absorption bands of many minerals is well documented (Burns, 1993). Comparatively little research has been conducted on soil minerals in this respect, however. As a result, much available information has been derived from either natural or synthetic pure mineral specimens.

The spectral features of the different minerals have usually been interpreted in light of the crystal field and ligand field theories. Specifically, differences among spectra for Fe minerals have been ascribed to distortions in $Fe(O, OH)_6$ octahedra or to differences in octahedral linkages, which alter the ligand field. Substitution of Al for Fe is a common source of such differences. For instance, the $^6A_1 \rightarrow {}^4T_1$ transition of synthetic goethite at ~950 nm shifts to a lower energy (longer wavelength) when Al enters its structure (Buckingham and Sommer, 1983; Scheinost et al., 1999b). This was ascribed to the decrease in Fe–(O, OH) distances caused by Al substitution, as also observed in synthetic hematite by Morris et al. (1992). Scheinost et al. (1999b) found Fe–(O, OH) distances to change by 0.2 pm, which, as noted by these authors, is one order of magnitude smaller than the sensitivity of extended X-ray absorption fine structure (EXAFS) spectroscopy. On the other hand, band positions and the degree of Al substitution in populations of natural minerals are not always related (Malengreau et al., 1997).

One other example of the use of diffuse reflectance spectroscopy to elucidate the structural properties of Fe oxides was provided by Gálvez et al. (1999), who worked with synthetic hematite prepared in the presence of phosphate. The presence of structural P in these hematites had been inferred from X-ray diffraction, IR spectroscopy, and acid dissolution studies. Diffuse reflectance spectra exhibited an absorption band typical of goethite (~488 nm) in addition to the typical hematite band (~538 nm). The "goethitic" component in hematite was proportional to the P content in hematite and was not observed in pure hematite with surface adsorbed phosphate. The previous evidence supports the hypothesis

that P is structural and probably occupies tetrahedral sites, which results in deficiency in the cationic substructure.

Isomorphous substitution by transition element cations (Co, Cr, Ni, Mn, V) in Fe oxides and other minerals markedly alters diffuse reflectance spectra, which provides valuable geochemical information. Thus, Scheinost (2000) reported the presence of several additional bands in the spectrum for goethite substituted by these elements due to M^{3+} crystal field transitions and M-to-Fe charge transfer. However, such effects are unlikely to be observed in soils unless they contain a high content in Fe oxides.

Diffuse reflectance spectroscopy has also been used to characterize nanometric surface precipitates. Thus, Scheinost et al. (1999a) studied secondary Ni precipitates on various silicates and gibbsite, and found the band for the $^3A_{2g} \rightarrow {}^3T_{1g}$ transition to be shifted to a shorter wavelength when the host mineral contained Al. This suggested that Al was dissolved from the sorbent and substituted for Ni in the brucite-like hydroxide layers of the precipitating phase, thus decreasing Ni–O distances and raising the crystal-field splitting energy.

Quantitative Analysis

Equation [11] is generally useful for quantitative analysis. Based on it, at any wavelength, the *K–M* function for a mixture of a small amount of a colored mineral in a matrix of white or colorless soil minerals (i.e., with very low *K* values) is proportional to, and depends almost exclusively on, the concentration of that mineral provided *S* is constant. Usually, *S* differs little among matrices of white or colorless soil minerals with a low percentage of the colored mineral. With higher concentrations, constancy of *S* can reasonably be approached in practice by diluting the sample with a "white" mineral or a white standard. If several colored minerals are present, then the *K–M* function is proportional to their *K* values as weighed according to their concentrations.

Quantitative analysis by Eq. [11] of even very small amounts of colored minerals can be accurate provided the *K* and *S* values for the colored minerals in the samples concerned are known. This is rarely the case, as it calls for an effective method to separate each mineral from the matrix and examine it separately. *K* and *S* are obtained by applying Eq. [13] to mineral–white standard mixtures. More often, the *K* and *S* values for external standards must be adopted. One is thus confronted with the fact that *K* and *S* (and color) for most minerals range widely as a function of their size, shape, and surface and crystal properties. This has been observed, for instance, in synthetic hematites and goethites (Barrón and Torrent, 1986), and in various natural and synthetic Fe oxides (Scheinost et al., 1998; Scheinost and Schwertmann, 1999). For mere comparison of samples from soils not differing markedly in properties, one can adopt average *K* and *S* values. Thus, Barrón and Torrent (1986) used a wide population of soils to obtain such average values for "soil" goethite and hematite.

Quantitative analysis can be performed by "inverting" Eq. [14] if the values of ρ_i, d_i, and w_i for each *i*th mineral are known (Clark, 1999). Quantitative analyses are also performed by measuring the intensity of the characteristic bands for each mineral in the *K–M* spectral curve or in the second-derivative curve. Thus, Scheinost et al. (1998) found the amplitudes of the typical goethite and hematite bands in the second-derivative curve to be proportional to the contents of these minerals when mixed with a deferrated matrix in a proportion less than about 2%. Increasing the proportion of any of these minerals beyond this level resulted in a less-than-proportional increase in band amplitude. As noted above, this saturation problem can be mitigated by diluting the sample with a white standard.

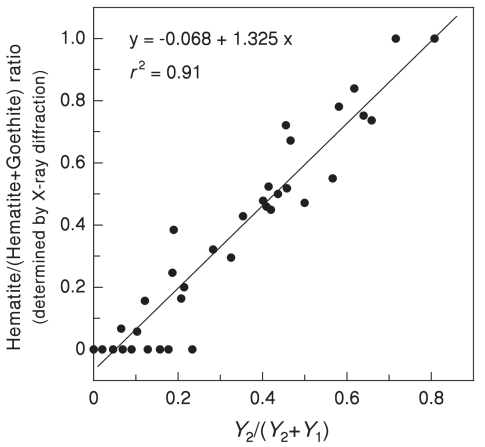

Fig. 13–5. Relationship between the hematite/(hematite + goethite) ratio as determined by differential X-ray diffraction and the ratio $Y_2/(Y_2 + Y_1)$ (Fig. 3) as determined by diffuse reflectance spectroscopy. Y_1 is the amplitude of the band between the minimum at ~415 nm and the maximum at ~445 nm, and Y_2 is the amplitude of the band between the minimum at ~535 nm and the maximum ~580 nm. Adapted from Scheinost el at. (1998).

Matrix effects on quantitative analyses make it advisable to estimate relative rather than absolute amounts of colored minerals in soils and mineral mixtures, provided the minerals exhibit characteristic, essentially nonoverlapping bands. For instance, many soils and sediments contain significant amounts of goethite and hematite as the only Fe oxides. On the basis of this, Scheinost et al. (1998) used the intensity of the second-derivative curve band between the ~415-nm minimum and the 445-nm maximum for goethite (denoted by Y_1 in Fig. 13–3), and that between the ~535-nm minimum and the 580-nm maximum for hematite (denoted by Y_2 in Fig. 13–3) to estimate the hematite/goethite ratio. Significant correlation was thus found between the hematite/(hematite + goethite) ratio and the $Y_2/(Y_1 + Y_2)$ ratio for a population of 40 soils with a wide range of properties (Fig. 13–5). Indeed, one can obtain the absolute proportions of two minerals for which the content ratio is known provided a method for determining the sum of the two contents exists. With goethite and hematite, the difference between the amounts of Fe extracted by the dithionite/citrate/bicarbonate mixture (Mehra and Jackson, 1960) and acid oxalate (Schwertmann, 1964) can be assigned to total Fe in both minerals.

Simple indices based on the various color notation systems have been used for more than 20 yr to estimate hematite content in soils, starting with the "redness rating" proposed by Torrent et al. (1980). The reader is referred to Torrent and Barrón (1993) for a description of such indices and their use. The indices have the advantage that color notation can be obtained either visually or with the aid of a tristimulus colorimeter, with no need to use a spectrophotometer to record the diffuse reflectance spectrum.

Acknowledgments

The authors acknowledge the financial support from Spain's CICYT within the framework of Project PB98-1015. Dr. A. Scheinost [European Synchrotron Radiation Facility (ESRF)] kindly revised an earlier draft of the manuscript.

REFERENCES

ASTM. 1973. Preparation of reflectance white standards. ASTM Standard E 259-66 (reapproved 1973). American Society for Testing and Materials, Philadelphia, PA.

Barrón, V., and J. Torrent. 1986. Use of the Kubelka–Munk theory to study the influence of iron oxides on soil colour. J. Soil Sci. 37:499–510.

Bedidi, A., B. Cervelle, J. Madeira, and M. Pouget. 1992. Moisture effects on visible spectral characteristics of lateritic soils. Soil Sci. 153:129–141.

Bell, J.F.I., H.Y.J. McSween, J.A. Crisp, R.V. Morris, S.L. Murchie, N.T. Bridges, J.R. Johnson, D.T. Britt, M.P. Golombek, H.J. Moore, A. Ghosh, J.L. Bishop, R.C. Anderson, J. Brückner, T. Economou, J.P. Greenwood, H.P. Gunnlaugsson, R.M. Hargraves, S. Hviid, J.M. Knudsen, M.B. Madsen, R. Reid, R. Rieder, and L. Soderblom. 2000. Mineralogical and compositional properties of Martian soil and dust: Results from Mars Pathfinder. J. Geophys. Res. 105:1721–1755.

Buckingham, W.F., and S.E. Sommer. 1983. Mineralogical characterization of rock surfaces formed by hydrothermal alteration and weathering—Application to remote sensing. Econ. Geol. 78:664–674.

Burns, R.G. 1993. Mineralogical applications of crystal field theory. 2nd ed. Cambridge Univ. Press, Cambridge, UK.

Commission Internationale de L'Eclairage. 1978. Recommendations on uniform color spaces, color-difference equations, psychometric color terms. Suppl. 2 to Publ. 15, Colorimetry. Bureau Central de la CIE, Paris.

Clark, R.N. 1999. Spectroscopy of rocks and minerals and principles of spectroscopy. p. 3–58. *In* A.N. Rencz (ed.) Manual of remote sensing. John Wiley & Sons, New York.

Clark, R.N., and T. Roush. 1984. Reflectance spectroscopy: Quantitative analysis techniques for remote sensing applications. J. Geophys. Res. 89:6329–6340.

Deaton, B.C., and W.L. Balsam. 1991. Visible spectroscopy—A rapid method for determining hematite and goethite concentration in geological materials. J. Sed. Pet. 61:628–632.

Duncan, D.R. 1940. The colour of pigment mixtures. Proc. Phys. Soc. 52:390–401.

Duncan, D.R. 1949. The colour of pigment mixtures. J. Oil Colour Chem. Assoc. 32:296–391.

Escadafal, R. 1989. Caractérisation de la surface des sols arides par observations de terrain et par télédétection. Editions de l'ORSTOM, Collections Études et Thèses, Paris.

Fernandez, R.N., and D.G. Schulze. 1987. Calculation of soil color from reflectance spectra. Soil Sci. Soc. Am. J. 51:1277–1282.

Gálvez, N., V. Barrón, and J. Torrent. 1999. Preparation and properties of hematite with structural phosphorus. Clays Clay Miner. 47:375–385.

Hapke, B. 1981. Bidirectional reflectance spectroscopy. 1. Theory. J. Geophys. Res. 86:3039–3054.

Hapke, B. 1993. Introduction to the theory of reflectance and emittance spectroscopy. Cambridge Univ. Press, New York.

Johnston, C.T., and Y.O. Aochi. 1996. Fourier transform infrared and Raman spectroscopy. p. 269–322. *In* D.L. Sparks (ed.) Methods of soil analysis. Part 3. Chemical methods. SSSA Book Ser. 5. ASA and SSSA, Madison, WI.

Kortüm, G. 1969. Reflectance spectroscopy. Springer-Verlag, Berlin.

Kosmas, C.S., N. Curi, R.B. Bryant, and D.P. Franzmeier. 1984. Characterization of iron oxide minerals by second-derivative visible spectroscopy. Soil Sci. Soc. Am. J. 48:401–405.

Kosmas, C.S., D.P. Franzmeier, and D.G. Schulze. 1986. Relationships among derivative spectroscopy, color, crystallite dimensions, and Al substitution of synthetic goethites and hematites. Clays Clay Miner. 34:625–634.

Kubelka, P. 1948. New contributions to the optics of intensely light-scattering materials. Part I. J. Opt. Soc. Am. 38:448–460.

Kubelka, P., and F. Munk. 1931. Ein Beitrag zur Optik der Farbanstriche. Z. Technol. Phys. 12:593–620.

Malengreau, N., J.-P. Muller, and G. Calas. 1995. Spectroscopic approach for investigating the status and mobility of Ti in kaolinitic minerals. Clays Clay Miner. 43:615–621.

Malengreau, N., P.G. Weidler, and A.U. Gehring. 1997. Iron oxides in laterites—A combined mineralogical, magnetic, and diffuse reflectance study. Schweiz. Mineral. Petrogr. Mitt. 77:13–20.

Mehra, P.O., and M.L. Jackson. 1960. Iron oxide removal from soils and clays by a dithionite-citrate system buffered with sodium bicarbonate. Clays Clay Miner. 7:317–327.

Morris, R.V., D.G. Schulze, H.V. Lauer, D.G. Agresti, and T.D. Shelfer. 1992. Reflectivity (visible and near IR), Mössbauer, static magnetic, and X-ray diffraction properties of Al-substituted hematites. J. Geophys. Res. 97:10257–10266.

Munsell Color. 1975. Munsell soil color charts. Munsell Color, Baltimore, MD.

Press, W.H., S.A. Teukolsky, W.T. Vetterling, and B.P. Flannery. 1992. Numerical recipes in Fortran. 2nd ed. Cambridge Univ. Press, Cambridge, UK.

SAS Institute. 1988. SAS/STAT user's guide. SAS Inst., Cary, NC.

Savitzky, A., and M.J.E. Golay. 1964. Smoothing and differentiation of data by simplified least squares procedures. Anal. Chem. 36:1627–1640.

Scheinost, A.C. 2000.Color. p. 27–42. *In* U. Schwertmann and R.M. Cornell (ed.) Iron oxides in the laboratory. Wiley–VCH, Weihheim, Germany.

Scheinost, A.C., A. Chavernas, V. Barrón, and J. Torrent. 1998. Use and limitations of second-derivative diffuse reflectance spectroscopy in the visible to near-infrared range to identify and quantify Fe oxides in soils. Clays Clay Miner. 46:528–536.

Scheinost, A.C., R.G. Ford, and D.L. Sparks. 1999a. The role of Al in the formation of secondary Ni precipitates on pyrophyllite, gibbsite, talc, and amorphous silica—A DRS study. Geochim. Cosmochim. Acta 63:3193–3203.

Scheinost, A.C., D.G. Schulze, and U. Schwertmann. 1999b. Diffuse reflectance spectra of Al substituted goethite: A ligand field approach. Clays Clay Miner. 47:156–164.

Scheinost, A.C., and U. Schwertmann. 1999. Color identification of iron oxides and hydroxysulfates: Use and limitations. Soil Sci. Soc. Am. J. 63:1463–1471.

Schwertmann, U. 1964. Differenzierung der Eisenoxide des Bodens durch Extraktion mit Ammoniumoxalat-Lösung. Z. Pflanzenernähr. Düng. Bodenkd. 105:194–202.

Sherman, D.M., and T.D. Waite. 1985. Electronic spectra of Fe^{3+} oxides and oxide hydroxides in the near IR to near UV. Am. Mineral. 70:1262–1269.

Simonson, R.W. 1993. Soil color standards and terms for field use—History of their development. p. 1–20. *In* J.M. Bigham and E.J. Ciolkosz (ed.) Soil color. SSSA Spec. Publ. 31. SSSA, Madison, WI.

Sunshine, J.M., C.M. Pieters, and S.F. Pratt. 1990. Deconvolution of mineral absorption bands: An improved approach. J. Geophys. Res. 95:6955–6966.

Torrent, J., and V. Barrón. 1993. Laboratory measurement of soil color: Theory and practice. p. 21–33. *In* J.M. Bigham and E.J. Ciolkosz (ed.) Soil color. SSSA Spec. Publ. 31. SSSA, Madison, WI.

Torrent, J., U. Schwertmann, and D.G. Schulze. 1980. Iron oxide mineralogy of some soils of two river terrace sequences in Spain. Geoderma 23:191–208.

USGS. 2003. Digital spectral library. Version 4: 0.2 to 3.0 microns. Available at http://speclab.cr.usgs.gov/spectral.lib04/spectral-lib04.html (accessed 12 Sept. 2003, verified 23 Mar. 2006).

Wendlandt, W.W., and H.G. Hecht. 1966. Reflectance spectroscopy. John Wiley & Sons, New York.

Wyszecki, G., and W.S. Stiles. 1982. Color science: Concepts and methods, quantitative data and formulae. 2nd ed. John Wiley & Sons, New York.